

See discussions, stats, and author profiles for this publication at: <https://www.researchgate.net/publication/309351527>

# High electron mobility transistor—a review on analytical models

Article · October 2016

CITATIONS

0

READS

45

2 authors, including:



[Dr. Vimala Palanichamy](#)

Dayananda Sagar Institutions

32 PUBLICATIONS 19 CITATIONS

[SEE PROFILE](#)

Some of the authors of this publication are also working on these related projects:



Physics Based Modeling Simulation and Electrical Characterization of Quantum Effects in Multigate MOSFETs [View project](#)



Analytical Modeling and Simulation of Triple Material Surrounding Gate (TMSG) TFET [View project](#)

All content following this page was uploaded by [Dr. Vimala Palanichamy](#) on 21 October 2016.

The user has requested enhancement of the downloaded file. All in-text references [underlined in blue](#) are linked to publications on ResearchGate, letting you access and read them immediately.

# High Electron Mobility Transistor: A Review on Analytical Models

**J. Shanthi**

*Assistant Professor*

*Department of Electronics & Communication Engineering  
AMC Engineering College, Bangalore, India*

**Dr. P. Vimala**

*Associate Professor*

*Department of Electronics & Communication Engineering  
Dayananda Sagar College of Engineering, Bangalore, India*

## Abstract

In recent years, high electron mobility transistors (HEMTs) have attracted much attention in high-speed and high-power applications. One of the most interesting properties of these devices is the formation of the two-dimensional electron gas (2-DEG) with a very high electron mobility at the hetero interface. AlGaAs/GaAs HEMTs have been and are promising candidates for high speed and mm-wave applications. GaN-based HEMTs have attracted much attention for application in high-frequency and high-power devices due to the large bandgap, high saturated electron velocity, and high breakdown electric field. Significant improvements in the fabrication and performance of high electron mobility transistors (HEMT) have stimulated a considerable interest in the modeling of such structures. In this paper, we review working principle and various structures of HEMT, also different analytical models available for HEMT.

**Keywords:** HEMT, MODFET, HFET, 2-DEG, Compact Model, Analytical Model, AlGaAs/GaAs, AlGaN/GaN, SG HEMT, DG HEMT, Tri-Gate HEMT, Nano Wire NCA HEMT, TCAD

## I. INTRODUCTION

The presence of an inversion or accumulation electron layer located at the interface hetero junctions was predicted by Anderson [1]. In 1969, Esaki and Tsu [2] proposed a hetero structure in which ionized impurities and free electrons could be spatially separated giving rise to a reduced Coulomb scattering. In 1978, Dingle *et al.* [3] observed mobility enhancement in modulation doped super lattices. A model describing C-V and I-V characteristics of modulation doped FET's is proposed by T.J.Drummond *et al.*, in 1982. In this model, the amount of charge transfer across the interface was found by equating the charge depleted from the AlGaAs to the charge accumulated in the potential well. A solution was then found such that the Fermi level is constant across the hetero-interface. Another important prediction of the model was the existence of the "subthreshold current" [4]. Kwyro Lee *et al.*, developed a model in 1983, which showed the change in the Fermi energy with the gate voltage changes the effective separation between the gate and the two dimensional electron gas by about 80 Å [5]. It has been found [6], [7] that the mobility of 2DEG electrons in the MODFET channel exceeds the mobility of electrons in bulk GaAs by more than an order of magnitude, in particular, when low-temperature conditions are applied. The 2-DEG charge transport through the channel is basically determined by the velocity-electric field characteristic, which is similar to that of Si rather than GaAs, but it exhibits a much higher saturation level. Naturally, if the problem of charge transport in the MODFET channel is to be treated in a rigorous manner, Schrodinger's and Poisson's equations must be solved simultaneously in order to obtain the device current-voltage characteristic. This approach, however, is not well suited for analytical modeling of the MODFET due to its complexity and it is preferable to use some analytic approximations that could lead to a reasonably accurate final solution.

A number of MODFET models that have been developed are based on linearization of the 2DEG charge versus channel voltage and they also neglect the aspects of the 2DEG charge density and mobility calculations. Consequently, a number of fitting parameters or so-called model constants are usually required to improve the inaccuracies resulting from these shortcomings [8]. One of the main limitations of many existing analytical high electron mobility transistor (HEMT) models is that they assume that the Fermi level in the quantum well is a linear function of the sheet carrier concentration  $n_s$  [9]. The first important analytical model of the HEMT was developed by Delagebeaudeuf and Linh in 1982 [10].

An important limiting feature of Delagebeaudeuf and Linh's model was that Fermi-level variation with electron density in the quantum well was neglected in order to get an analytical model. If it is accounted for, then a few equations related to the model must be solved numerically [9]. An-Jui *et al.*, [11] developed a simple but more accurate nonlinear charge control model, which was derived directly from the triangular potential well approximation.

The paper is arranged as follows: The working principle of HEMT is described in section II. Various HEMT versions and structures are described in section III and IV. Then analytical models of HEMTs are reviewed and followed by conclusion in section V and VI respectively.

## II. WORKING PRINCIPLE OF HEMT

In the vicinity of a semiconductor heterojunction electrons are transferred from the material with the higher conduction band energy  $E_c$  to the material with the lower  $E_c$  where they can occupy a lower energy state. This can be a large number of electrons especially if the semiconductor with the high  $E_c$  barrier is doped. Near the interface a two dimensional electron gas (2DEG), the channel is created. This way it is possible to separate the electrons in the channel from their donor atoms which reduces Coulomb scattering and hence increases the mobility of the conducting electrons are penetrating into the buffer under the channel very easily where their mobility is usually lower and the control of the gate is poor. To keep the electrons in the channel a second energy barrier below the channel can be introduced by a material with a higher  $E_c$  than the channel material.

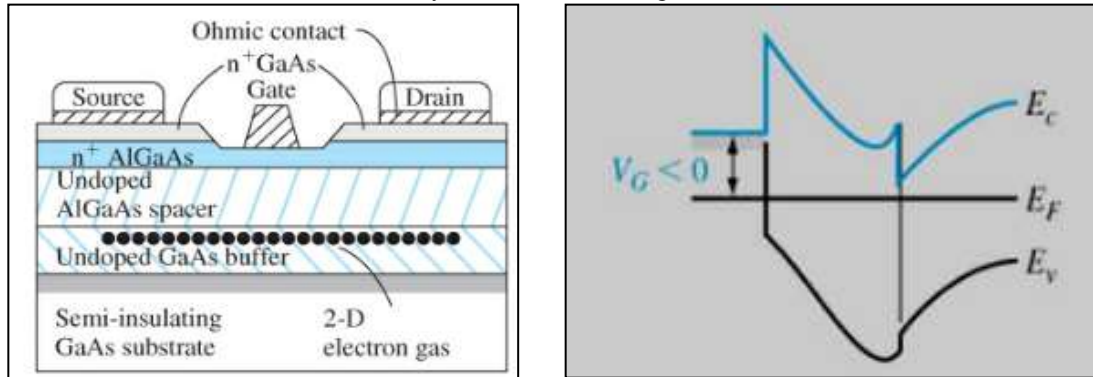


Fig. 1: AlGaAs/GaAs HEMT Structure and its conduction energy band diagram

The conduction band energy under the gate is shown in above Fig. 1, the conduction band of the channel relative to the Fermi level  $E_f$  is determined by  $\Delta E_c$ , the doping level  $N_D$ , the barrier height of the schottky contact  $q\phi_B$ , the gate to channel separation  $d_{GC}$ , and the applied voltage on the gate  $V_g$ . To obtain high drain currents  $I_d$  and high transconductance  $g_m$  it is favorable to maximize  $q\phi_B$ ,  $N_D$ ,  $\Delta E_c$ , and to minimize  $d_{GC}$ . If homogeneously doped upper barrier layer is used  $q\phi_B$ ,  $N_D$  and  $d_{GC}$  are directly related to each other. A decrease in  $d_{GC}$  reduces the total doping in the barrier layer which shifts the Threshold voltage ( $V_t$ ) to more positive values and thus reduces  $I_{d,max}$ . If  $N_D$  is increased  $\phi_B$  of the Schottky contact is reduced.

## III. DIFFERENT STRUCTURES OF HEMT

### A. AlGaAs/GaAs HEMT

The top layer n plus source contact, n plus drain contact, and doped aluminum gallium arsenide. That is equivalent of the MESFET, but it is disabled here by putting a gate on this, which actually depletes the entire layer. If it is depleted that and also, if it has this doped aluminum gallium arsenide on the gallium arsenide, there would be a two-dimensional electron gas [2DEG] here. It is actually these electrons that are actually used for current transport and to ensure that this layer (the top layer, heavily doped layer) does not participate in the conduction of any portion of the device operation.

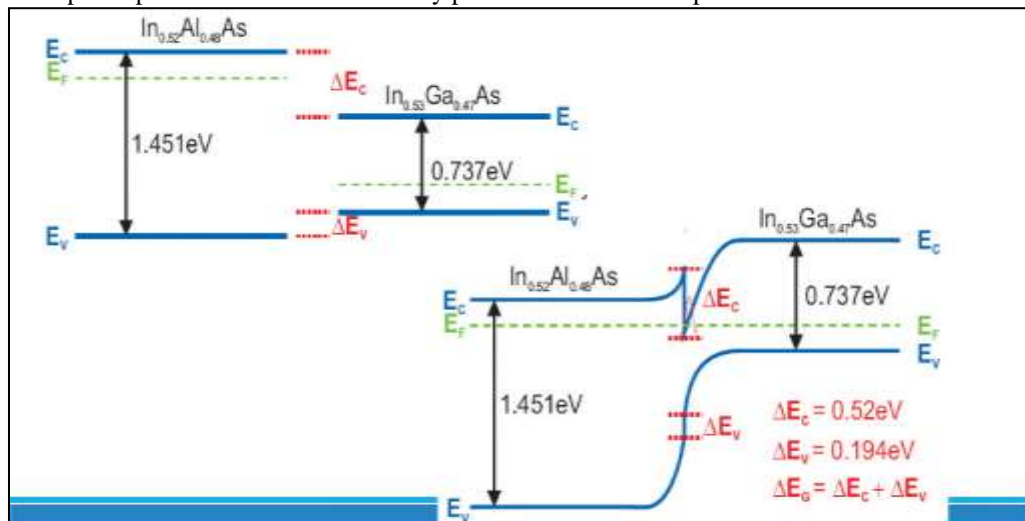


Fig. 2: Band energy diagram of HEMT

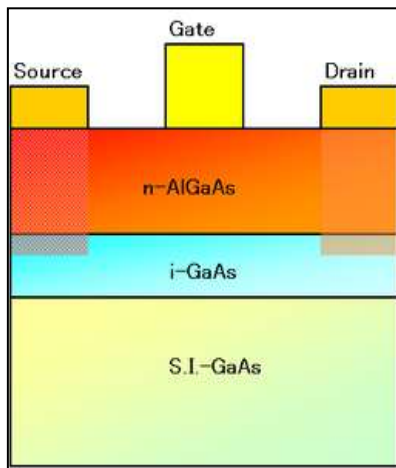


Fig. 2: Structure of AlGaAs/GaAs HEMT

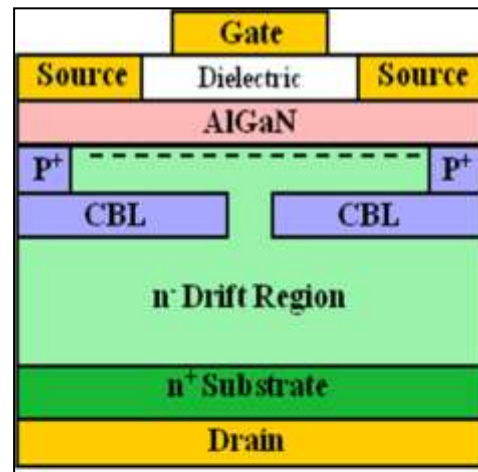


Fig. 3: Schematic of a vertical GaN HEMT

### B. AlGaAs/GaN Structure

The basic concept in a HEMT (Fig.4) is the aligning of a wide and narrow band gap semiconductor adjacent to each other to form a heterojunction. The carriers from a doped wide energy gap material (AlGaAs) diffuse to the narrow band gap materials (GaN) where a dense 2-DEG (Two Dimensional Electron Gas) is formed in the GaN side but close to the boundary with AlGaAs. The unique feature of the HEMT is channel formation from carriers accumulated along a grossly asymmetric heterojunction, i.e. a junction between a heavily doped high band gap and a lightly doped low band gap region. To achieve proper operation of the device, the barrier layer  $\text{Al}_x\text{Ga}_{1-x}\text{N}$  must be at a higher energy level than the conduction band of the GaN channel layer. This conduction band offset transfers electrons from the barrier layer to the channel layer. The electrons that are transferred are confined to a small region in the channel layer near the hetero-interface. This layer is called the 2DEG (Fig.4) and a defining characteristic of the HEMT. There are many factors that determine the quality of the 2DEG. The Fermi energy level of this thin layer is above the conduction band thereby making the channel highly conductive. The ratio of aluminum to gallium in AlGaAs is typically 30% Al and 70% Ga. The resulting compound has a higher energy band gap and different material properties from GaN. The structure of HEMT is formed by various layers via nucleation, buffer, spacer, carrier supply, barrier and cap layers. In a typically doped AlGaAs/GaN HEMT structure, AlGaAs donor (carrier supply) layer supplies electrons to the 2DEG. The 2DEG is formed at the AlGaAs/GaN interface even if all the layers are grown without intentional doping. In fact the contribution of the doping to the 2DEG sheet carriers concentration is reported to be less than 10% due to stronger piezoelectric effect in the material system. The polarization induced charges present in the hetero-interface induce a layer of two dimensional electron gas (2DEG) in the GaN layer immediately under the interface causing significant effects on current and other parameters.

### C. Indium Phosphide (InP) Structure

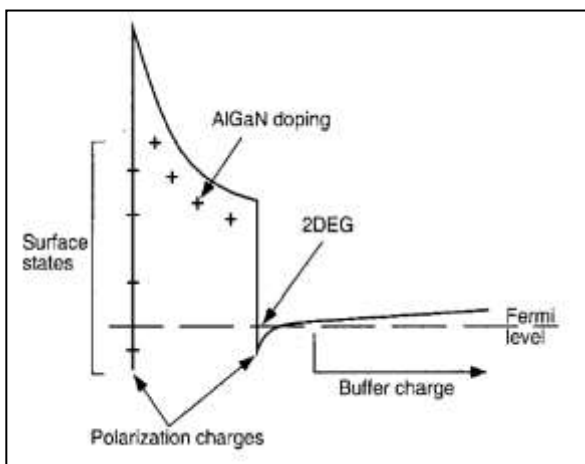


Fig. 4: Energy band diagram showing 2DEG formation.

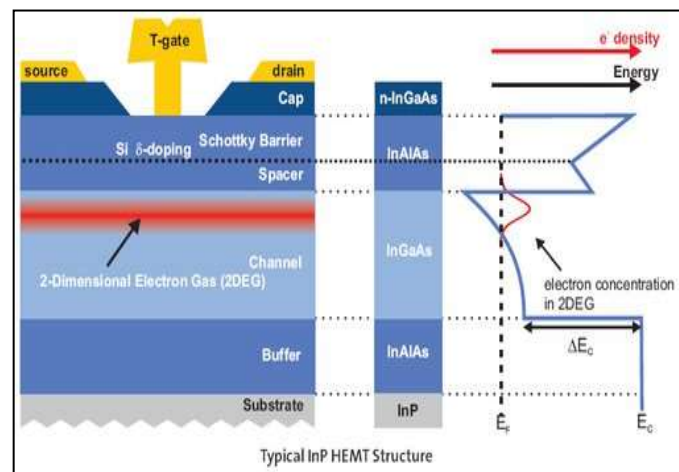


Fig. 5: Structure of InP HEMT

When compared to conventional gallium arsenide-based (GaAs) high electron mobility transistors (HEMTs), indium-phosphide-based (InP) HEMTs result in lower electron effective mass in the indium gallium arsenide (InGaAs) channel layer. InP-HEMTs also feature a relatively large conduction band offset (approximately 0.5 eV) between the channel layer and adjacent barrier layer

(indium aluminum arsenide, InAlAs). Therefore, InP-HEMTs are characterized by high electron mobility, high electron saturation velocity, and high electron concentration.

To enhance the high-speed and low-noise characteristics of HEMTs, it is necessary to increase the electron mobility in the channel. Above Fig shows a structure of InP HEMT. Its channel features an In(0.53)Ga(0.47)As composition with a percentage composition of InP: (In+Ga)=53% that achieves twice the electron mobility of GaAs. In view of the high percentage of indium in this composition, the lattice is matched to that of the InP substrate to achieve a stable crystal quality and consequent good electrical performance. In general, InP HEMTs have an InGaAs channel layer and InAlAs supply layer grown on the InP substrate. InP-based high electron mobility transistors (InP HEMTs) exhibit a record current-gain cutoff frequency of frequency of beyond 500GHz and an ultra-low noise figure of less than 2dB even at 100GHz. Consequently they are regarded as key devices for next-generation wired/wireless communication systems and precision sensors.

The structure of InP HEMT is shown in Fig. 5. The governing principles behind any improvement in the high-speed performance of an HEMT consist of reducing the traveling distance of electrons—the gate length—and increasing the traveling speed. The electron beam (EB) lithography technology is used to fabricate a T-shaped gate electrode with a gate length of less than 50 nm. Since the T-shaped gate enables the reduction of gate length while maintaining a large cross-sectional area, gate resistance can be minimized. The top and middle layers were exposed simultaneously at a relatively low dose and then developed with a high-sensitivity developer. The bottom layer was then exposed at a relatively high dose and developed with a low-sensitivity developer. Since the dimensions of the ultra-fine pattern on the bottom layer determine the gate length of the T-shaped gate, it is essential to fabricate, with high precision, an ultra-fine pattern of less than 50 nm.

#### IV. MODELS OF HEMT

##### A. 2D Analytical Model for I-V Characteristics

In 2008, for the first time, Miao Li et al [13] improved the conventional charge control model by employing the Robin boundary condition when solving the 1-D Schrödinger equation in the low longitudinal-field region and introducing an adjustable eigen value during the solution of the 2-D Poisson's equation in the velocity-saturation region. They also developed a modified Polyakov-schwierz Mobility model as well as a low field mobility model.

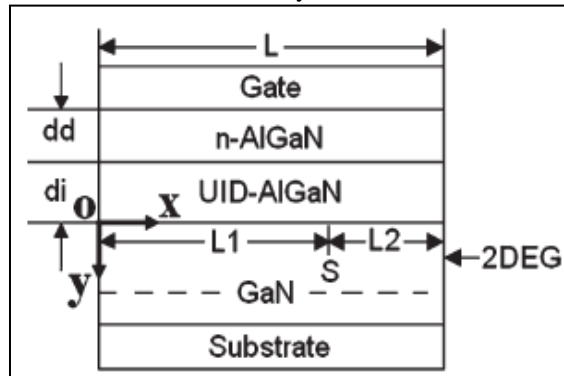


Fig. 6: Cross-sectional view of an AlGaIn/GaN MODFET with gate length  $L$ , n-AlGaIn layer thickness  $dd$ , and spacer layer thickness  $di$ . [13].

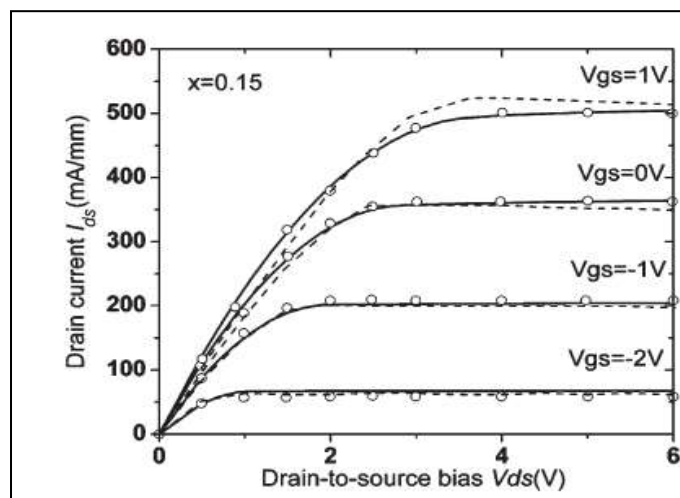


Fig. 7: Calculated and measured  $I$ - $V$  characteristics for an Al<sub>0.15</sub>Ga<sub>0.85</sub>N/GaN MODFET. [22] (dash line) and experimental data [23] (symbol).



The authors also plotted the variation of drain current  $I_{ds}$  with drain to source voltage  $V_{ds}$  for an Al<sub>0.15</sub>Ga<sub>0.85</sub>N/GaN and Al<sub>0.50</sub>Ga<sub>0.50</sub>N/GaN MODFETs. In their calculations the gate to source bias is swept from 1 to -2V at a step of -1V for Al<sub>0.15</sub>Ga<sub>0.85</sub>N/GaN and the same is swept from 2 to -3 v at a step of -1V for Al<sub>0.50</sub>Ga<sub>0.50</sub>N/GaN as shown in fig (7),(8) and also it is compared with the earlier models.

### B. Surface Potential based Analytical Model

Sourabh Khandelwal et al [14], developed a model accounts for the interdependence  $E_f$  and Fermi level  $\eta_s$ . Also they developed this model by considering the variation of  $E_f$ , the first subband  $E_0$ , the second sub band  $E_1$  and  $\eta_s$  with applied gate voltage  $V_g$ . They have developed this model by simplifying basic device equations in different regions of operation and combining them. In this model, the authors considered two regions with respect to  $E_0$  value. The regions are named as Region I where  $E_0$  is larger than  $E_f$  and Region II where  $E_0$  is lower than  $E_f$ . First, they developed models for  $\eta_s$  separately in regions I and II. Then, by combining two regional models' expressions they developed a unified model for charge density and they compared those with numerical calculations as shown in figure 9.

### C. Surface Potential-based Terminal Charge and Capacitance Model

Aixi Zhang et al [24], developed a surface potential based terminal charge and capacitance model including parasitic components for AlGaIn/GaN HEMT in 2014. They developed this model by using the following Algorithm:

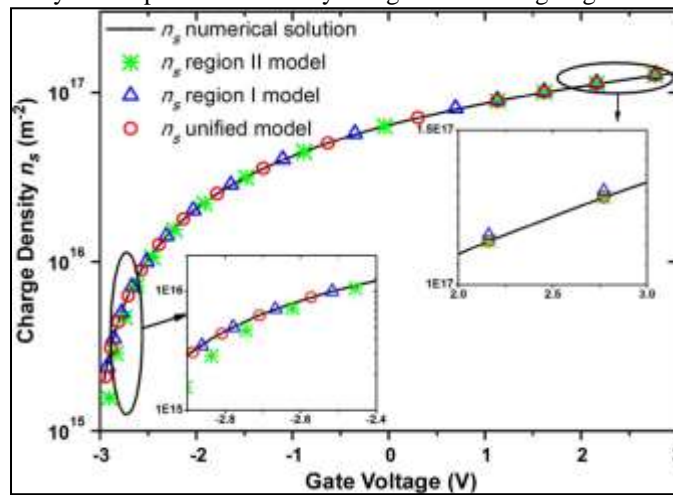


Fig. 9: Comparison of numerical calculations and the unified and regional analytical models of  $n_s$  versus gate voltage.  $T = 298$  K. [14].

- 1) Solving the charge control equations to determine the sheet charge density in the channel.
- 2) The intrinsic terminal charges and capacitances are derived consistently with current model.
- 3) Finally, the capacitances for the full structure of the HEMT devices are modeled by introducing parasitic components. The model gives the three terminal charges and nine intrinsic transcapacitances, after the close-form modeling of sheet charge density. They also evaluated their model by using TCAD simulations.

The following figure explains their proposed capacitance schematics for an AlGaIn/GaN HEMT with donor-like surface traps and acceptor-like bulk traps at both OFF-state and ON-state.

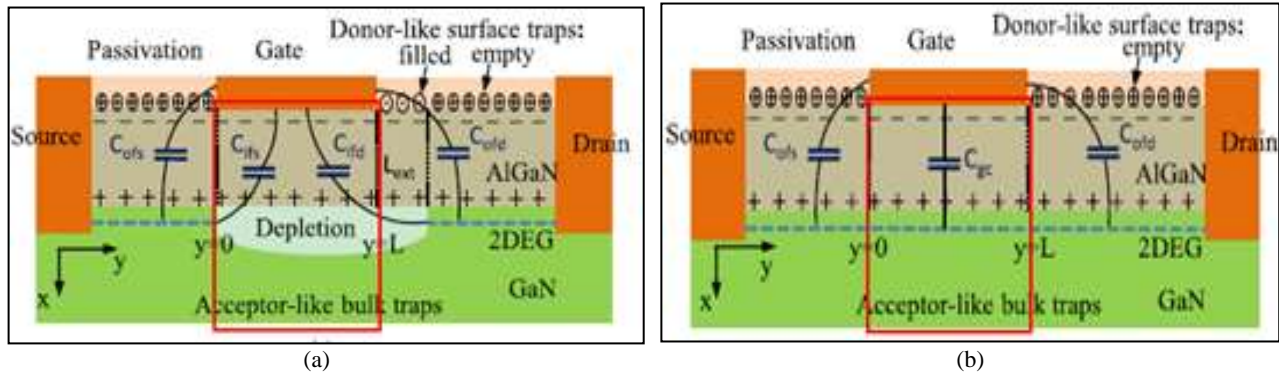


Fig. 10: Cross-sectional schematics of an AlGaIn/GaN HEMT and its capacitance partition, including the intrinsic capacitance and inner fringing and outer fringing capacitances of (a) off-state and (b) on-state. The donorlike surface traps and acceptor-like bulk traps are sketched. The core parts of the devices are highlighted by the red boxes. The extended length  $L_{ext}$  accounts for the extended depletion region induced by the electrons injection to the surface traps [25], [26], which affects fringing capacitances.

They also compared their model with TCAD simulations and numerical results of sheet charge density versus gate voltage at  $T=300\text{K}$  as shown in figure 11.

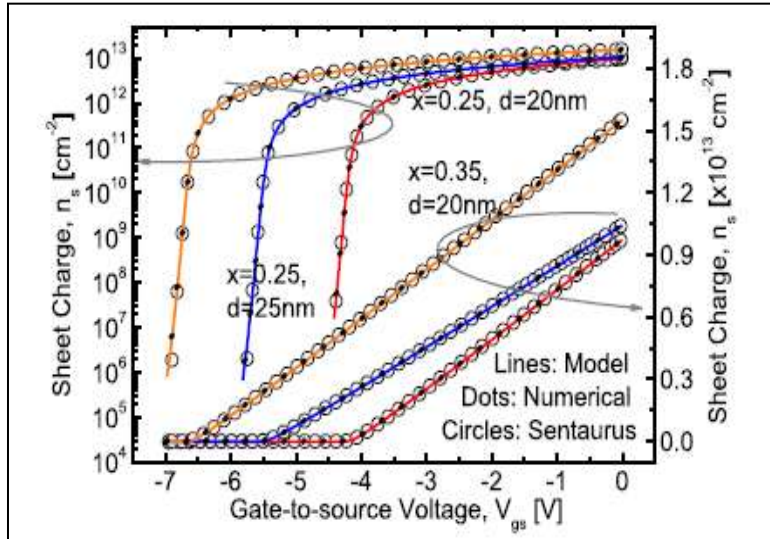


Fig. 11: Comparison of analytical models, TCAD simulations, and numerical results of sheet charge density versus gate voltage at  $T = 300\text{ K}$ .  $x$  is AlN mole fraction in AlGaIn layer. The numerical results are obtained by solving the (1)–(3) iteratively.[24]

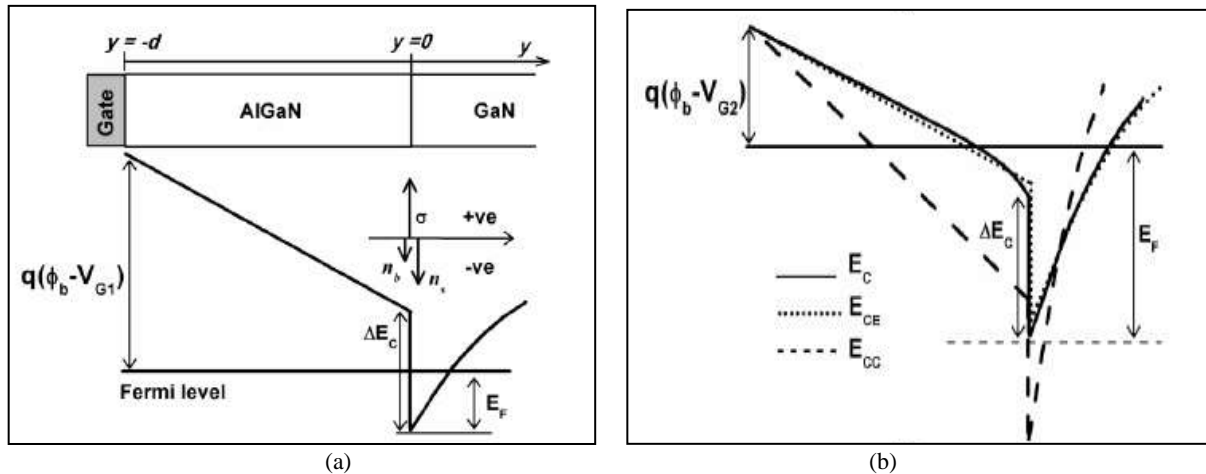


Fig. 12: Typical structure, charge distribution, and actual CBE diagrams (solid line) for Ga face AlGaIn /GaN HEMT at (a) low-to-moderate gate bias and (b) high gate bias, and approximate profiles considering electric fields from (1) (dashed line) and (2) (dotted line)[16].

#### D. An Analytical Model for 2DEG Charge Density

Naveen Karumari et al, developed a model in 2014 [16], which has a special feature of the inclusion of electron charges in the AlGaIn barrier layer within an analytical framework using an approximation of the Fermi–Dirac integral function. This model is therefore able to correctly predict the saturation of  $n_s$  at high  $V_G$ , unlike earlier models which ignore the electron charges in the AlGaIn layer.

This model is valid for the entire range of operation from subthreshold to practical forward biases. The model is validated by excellent match with results from numerical self-consistent simulations for a wide range of thickness, doping concentration, and Al mole fraction in the AlGaIn layer.

They calculated sheet charge density for three different regions where  $E_f < E_0$ ,  $E_0 < E_f < \Delta E_c$  and  $E_f > \Delta E_c$ . All these three expressions are unified to obtain a single expression valid for  $V_g \geq V_{off}$  and  $V_g \leq V_{off}$ . also, the model is validated by a numerical finite difference method (FDM)-based self-consistent Poisson-Schrodinger solver and it is plotted as shown in figure 13.

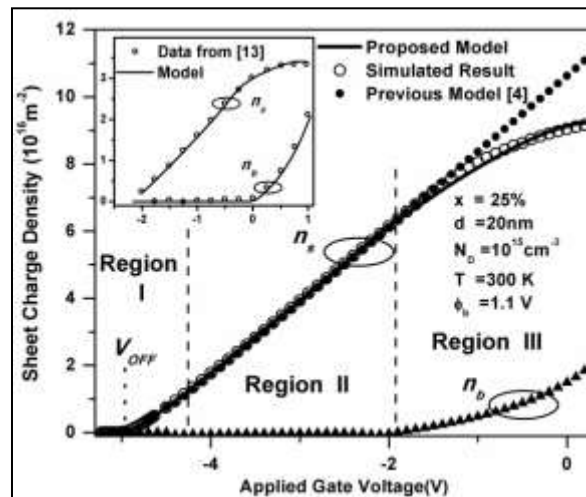


Fig. 13: Comparison of 2-DEG electron density ( $n_s$ ) from the proposed model (solid line) with that from numerical FDM solver ( $^{\circ}$ ) and from [4] ( $\bullet$ ). [16] The variation of electron density in AlGaIn barrier ( $n_b$ ) is also shown. Inset: compares results from our model with data from [27].

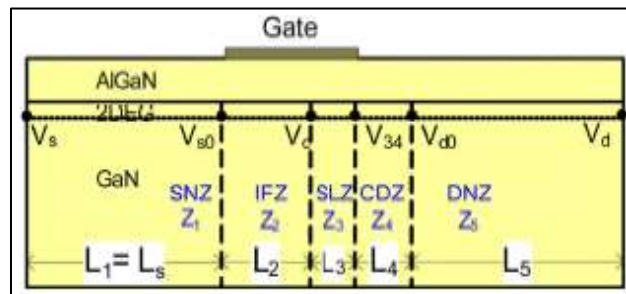


Fig. 14: Previous five-zone HFET model from [3]. The origin  $x = 0$  is at the left-most edge  $v = V_s = 0$  of the source access region. The right-most edge  $x = L_s + L_g + L_d = L_1 + L_2 + L_3 + L_4 + L_5$  of the drain access region is at  $v = V_d$ . [15].

### E. A Five Parameter Model

In 2015, Griff L. Bilbro et al [15], derived drain current of an AlGaIn/GaN HFET based on five parameters, which can be expressed in terms of geometry and materials of a device. The presently proposed model is intended to:

- Interpolate between designs for measured devices
- Extrapolate changes of performance that result from a change in the geometric or material design of a measured device
- Be simple enough to intuitively relate device operation to device design; and
- Predict the sensitivity of the operation of a device to changes in its design.

### F. Surface Potential Based Compact Model

Sudhip ghosh et al, developed an analytical model for the gate current in AlGaIn/GaN HEMT for the first time in 2015 [17]. This gate current model is implemented to calculate the PF current equations, the electric field expression is obtained in terms of  $\psi$ . They also proved that the developed model is in excellent agreement with experimental gate-current at multiple drain voltages and temperatures.

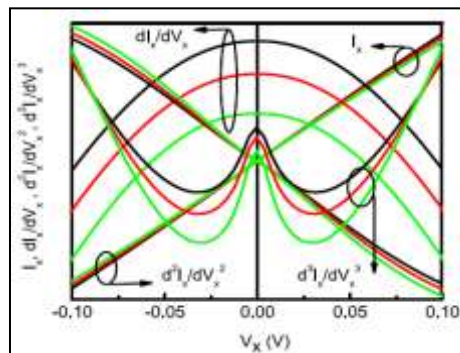


Fig. 15: Gummel symmetry test,  $I_x$  and its derivatives up to third orders with respect to  $V_x$ , where  $V_x = V_{ds}/2$  and  $V_d$  and  $V_s$  are swept in opposite directions. [17].



The authors also proved that the model passes the Gummel Symmetry test. the proposed model is symmetric around  $V_{ds} = 0V$ , it is smooth and continuous.

### G. Physics Based Compact Model

Sourabh Khandelwal et al in 2012 presented a physics based model, which is derived from a consistent solution of Schrodinger's and Poisson's equations [18].

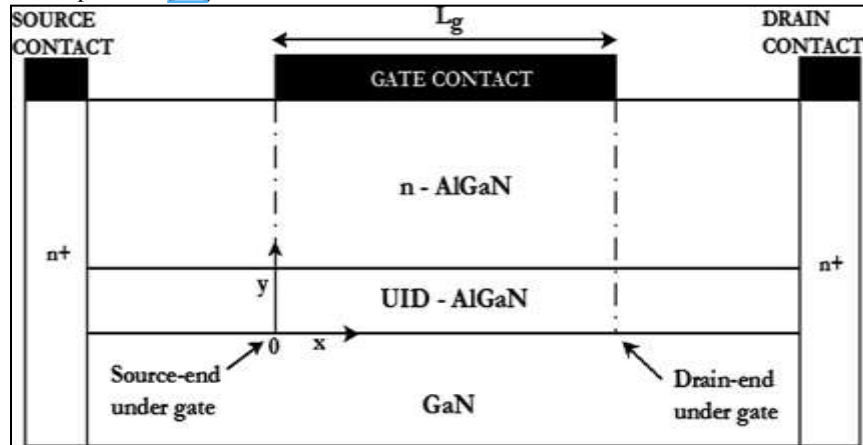


Fig. 16: Cross sectional view (not drawn to scale) of AlGaIn/GaN HEMT. UID is a thin un-intentionally doped AlGaIn layer commonly used for mobility enhancement.[18].

The authors treated the source-gate and drain-gate gap regions as parasitic resistances and developed drain current and capacitance models. They also compared their model with the earlier models and the same is presented as shown in Fig.17.

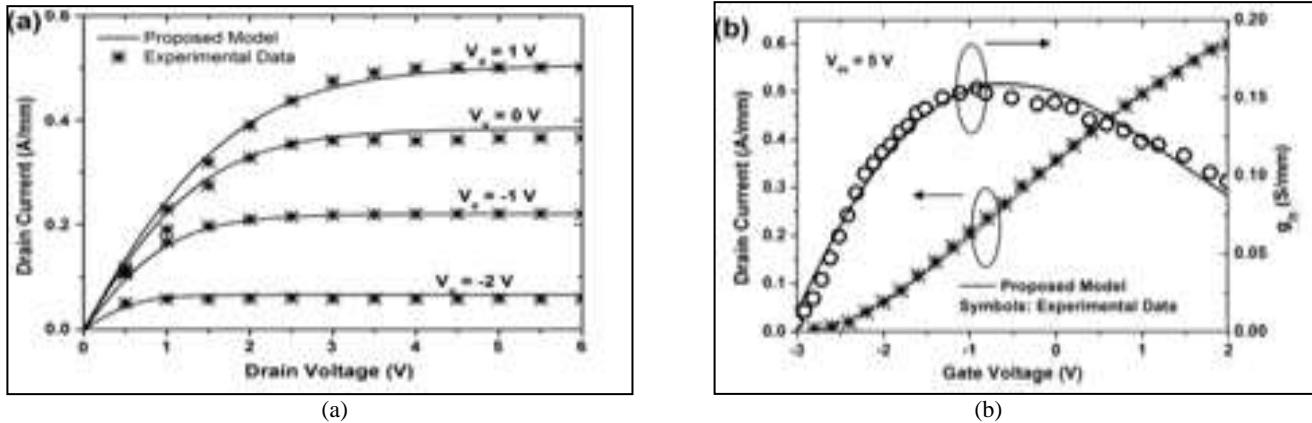


Fig. 17: Comparison of the modeled (a)  $I_d$ - $V_d$  and (b)  $I_d$ - $V_g$  and  $g_m$ - $V_g$  DC characteristics with the experimental data for  $Al_{0.15}Ga_{0.85}/GaN$   $L_g = 1 \mu m$  device [18]. Experimental data is taken from [28].

### H. InGaAs/InAlAs HEMT Structure

N.A.Yuzeeva et al [19] investigated the influence of In content on the electron mobilities and effective masses in dimensionally quantized subbands. They also stated that most of the HEMT structures on InP substrates have an InGaAs channel since high electron mobility could be achieved in this material especially with increasing In content due to the reduction of the effective electron mass [20, 21]. They concluded that the highest electron mobility was observed in sample with the highest In content and corresponds to a lower electron effective mass.

#### I. AlGaIn/GaN Double Gate HEMT

In DGHEMT, same layers of SGHEMT except the buffer layer were used both at up and down sides. The fabrication of DGHEMT is possible by using transfer substrate technique.[31]. DGHEMT offers numerous advantages over conventional single-gate HEMT (SGHEMT), such as counteracting the effect of carriers injection into the buffer, since no buffer is used in DGHEMT that provides better charge control over SGHEMT. DGHEMT also exhibits a better pinch-off behavior, lower output conductance and higher transconductance ( $g_m$ ) [29].

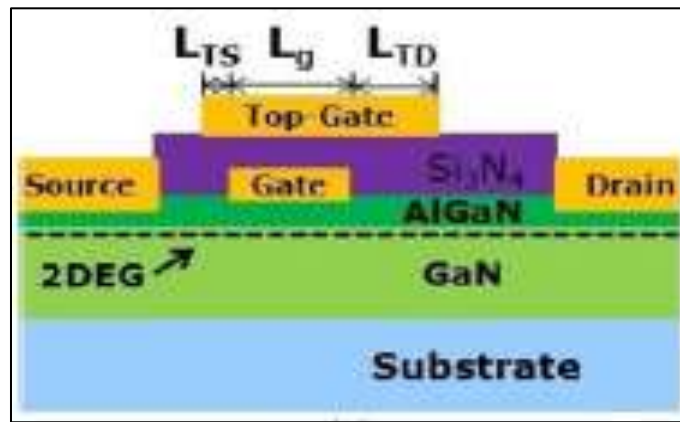


Fig. 18: Schematic cross-sectional diagram of an AlGaIn/GaN DG-HEMT.[30]

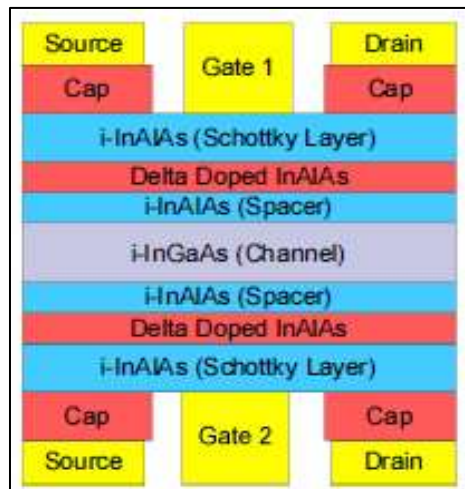


Fig. 19: 2D cross sectional view of DGHEMT.[31]

Guohao et al.(2013) proposed and fabricated a novel AlGaIn/GaN Double Gate HEMT (DGHEMT) as shown in figure.18.[30].This new device structure, has an additional top gate electrode which covers the normal gate and extends to source and drain electrodes with overhangs. The overhangs' lengths are expressed as  $L_{TS}$  (in the direction pointing to the source) and  $L_{TD}$ (in the direction pointing to the drain), respectively. The authors also investigated dynamic performances by the effects of SFP (Source Field Plate) and GPF (Gate Field Plate) by applying additional pulse signal on the top gate. Finally, they concluded that the GFP improves dynamic performances more than the SFP did, because of the following two reasons: 1).The 2DEG compensation during the ON-state, and 2).The other is less negative charge trapping during the OFF-state.

#### J. InAlAs/InGaAs DGHEMT

Zafar et al (2013) presented InAlAs/InGaAs DGHEMT for THz frequency range. They designed this structure with 50nm gate length to reduce the short channel effect as well as enhance the cut-off frequency as shown in Figure.19.

They have taken a SGHEMT with  $L_g=300\text{nm}$  as a reference device to model their proposed DGHEMT with  $L_g=50\text{nm}$ . They also showed the comparison of those two device characteristics of by using TCAD software as shown in Table-1.

Table – 1  
Comparison of designed SGHEMT and DGHEMT [31]

Device Characteristics	SGHEMT		DGHEMT $L_g = 50\text{nm}$
	$L_g = 300\text{nm}$	$L_g = 100\text{nm}$	
$g_m$ (S/mm)	0.91	0.86	1.81
$g_d$ (S/mm)	0.08	0.09	0.09
Unloaded voltage gain	11.38	9.56	20.11
$C_T$ (pF/mm)	1.22	0.87	1.62
$f_T$ (GHz)	108	144	175
$f_{max}$ (GHz)	349	432	448

They concluded that DGHEMT devices are an ideal and suitable candidate for future THz applications. By implementing DGHEMT structure, 62% enhancement in  $f_T$  and 28.3% enhancement in  $f_{max}$  are achieved w. r. t their reference structure of 300nm SGHEMT [31].

#### K. Nano Wire Channel HEMT

One of the critical issues is the nonlinear behavior of short-channel GaN HEMTs. In conventional GaN devices, the extrinsic transconductance ( $g_m$ ) drops quickly with increasing drain current after reaching its peak value, and this issue becomes more serious as the gate length scales down [32]. Dong Seup Lee et al [32], reported a high linearity InAlN/GaN high electron mobility transistor (HEMT) with a nano wire channel structure in the year 2013. The authors demonstrated a nanowire channel InAlN/GaN HEMTs with high linearity of both  $g_m$  and  $f_T$ . They formed the nano wire channels only under the gate, while maintaining a planar structure in the access region, the source access region resistance was maintained well below that of the channel and remain linear even at high channel currents, which allowed high linearity characteristics. Also, they found that the suppression of the increase in the source resistance allowed a higher drain current drivability of the intrinsic GaN HEMTs.

The authors also compared the dc transfer and output characteristics of the  $L_g = 70\text{--}80\text{-nm}$  nanowire channel device with the conventional planar transistor as shown in Fig.21. It is found that the nano wire channel device has much flatter extrinsic transconductance ( $g_m$ ) than the planar device because of the relatively larger current drivability of its source access region.

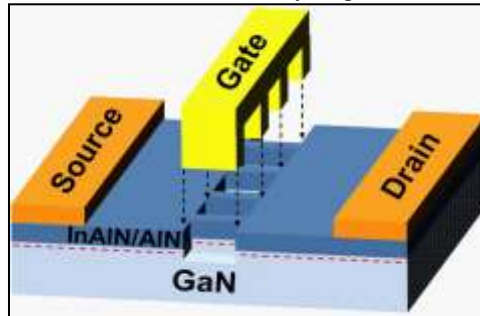


Fig. 20: Device structure of nanowire channel HEMT [32].

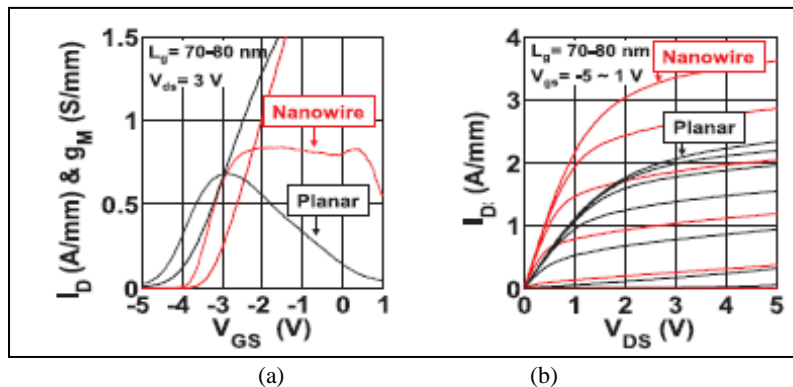


Fig. 21: Comparison of dc (a) transfer and (b) output characteristics of  $L_g = 70\text{--}80\text{-nm}$  nanowire channel device.

#### L. Tri-Gate AlGaIn/AlN/GaN HEMTs

Wael Jatal et al, demonstrated the device called tri-gate HEMTs based on an  $\text{Al}_{0.2}\text{Ga}_{0.8}\text{N}/\text{AlN}/\text{GaN}$ -heterostructures in the year 2016. This heterostructure was grown on Si substrates using an ultrathin SiC transition layer. The growth of the  $\text{Al}_{0.2}\text{Ga}_{0.8}\text{N}/\text{AlN}/\text{GaN}$ -heterostructures on 3C-SiC (111)/Si (111) was performed using metal organic chemical vapour deposition (MOCVD), [33] which is similar to [32]. In this paper, they reported about the fabrication of E-mode and D-mode AlGaIn/AlN/GaN HEMTs on Si substrates using a SiC transition layer. The Structure of the fabricated NCA HEMT is shown in Fig. 22.



Fig. 22: The optical microscopic image of NCA HEMT structure. [33]

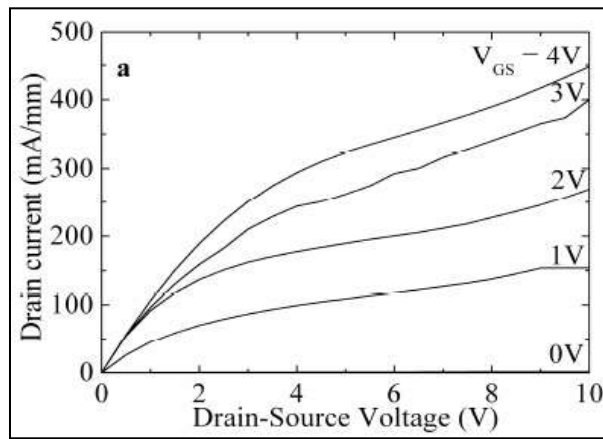


Fig. 23: Output characteristics of NCA HEMT structure with 200nm gate length.[33]

The authors plotted the output and transfer characteristics of NCA HEMT as shown in Fig.23 and 24 respectively. From the plots, we infer that the output characteristics exhibited good saturation, since the maximum drain current densities  $I_{DS}$  was 445mA/mm for  $V_{GS} = 4V$  and a drain-source voltage of  $V_{DS} = 10V$ . The extrinsic transconductances  $g_m$  reached values of 235 mS/mm at  $V_{DS}=5V$  for Al<sub>0.2</sub>Ga<sub>0.8</sub>N/AlN/GaN-heterostructures as shown in Fig.24. Also, they found that the breakdown voltages of the fabricated NCA HEMT was 300V [33].

## V. CONCLUSION

A detailed review on different structures and models of High Electron Mobility Transistor is done in this paper. The HEMT models that are analysed in this paper are 2-D analytical model for I-V characteristics, Surface potential based analytical model, Surface potential-based terminal charge and capacitance model, An analytical model for 2DEG charge density, A Five parameter Model, Surface Potential Based Compact Model, Physics Based Compact Model and InGaAs/InAlAs HEMT structure. All these models were developed based on the parameters governing the performance and operation of HEMT like 2-DEG charge density, sheet charge density, drain current, surface potential etc. All the related parameters are calculated from the solution of Schrodinger's and Poisson's equations in the quantum well assuming a triangular potential profile. Also these models are in excellent agreement with experimental data and validated by using TCAD simulator. Apart from all those normal or SGHEMT structures, we also reviewed few DGHEMT structures such as AlGaIn/GaN DGHEMT, InAlAs/InGaAs DGHEMT. Indeed, the DGHEMT structures have numerous advantages over SGHEMT. In addition, we also reviewed the structure and characteristics of two recently developed structures like nano wire channel HEMT and nano channel array Tri Gate HEMT in this paper.

## REFERENCES

- [1] R. L. Anderson, "Germanium-gallium-arsenide heterojunctions," IBM J. Res. and Develop., vol. 4, pp. 283-287, 1960.
- [2] L. Esaki and R. Tsu, "Superlattice and negative conductivity in semiconductors," IBM Res., Internal Rep. RC 2418, Mar. 26, 1969.
- [3] R. Dingle et al., "Electron mobilities in modulation-doped semiconductor heterojunction superlattices," Appl. Phys. Lett., vol. 33, pp. 665-667, Oct. 1978.
- [4] T. J. Drummond, H. Morkog, K. Lee, and M. S. Shur, "Model for modulation-doped field-effect transistor," IEEE Electron Device Lett., vol. EDL-3, p. 338, 1982.
- [5] K. Lee, M. Shur, T. J. Drummond, and H. Morkog, "Current-voltage and capacitance-voltage characteristics of modulation-doped field-effect transistors," IEEE Trans. Electron Devices, vol. ED-30, pp. 207-212, 1983.
- [6] H. L. Stormer, A. Pinczuk, A. C. Gossard, and W. Wiegmann, "Influence of an undoped (AlGa)As spacer on mobility enhancement in GaAs-(AlGa)As superlattices," Appl. Phys. Lett., vol. 39, no. 9, pp. 691-693, May 1981.
- [7] H. L. Stormer, A. C. Gossard, W. Wiegmann, and K. Baldwin, "Dependence of electron mobility in modulation-doped GaAs-(AlGa)As heterojunction interfaces on electron density and Al concentration," Appl. Phys. Lett., vol. 39, no. 11, pp. 912-914, Dec. 1981.
- [8] Marian L. Majewski, "An Analytical DC model for the Modulation Doped Field Effect Transistor," IEEE Trans. Electron Devices, vol. ED-34, No. 9, Sep-1987.
- [9] S. Kola, J. M. Goloio, and G. N. Maracas, "An analytical expression for Fermi level versus sheet carrier concentration for HEMT modeling," IEEE Electron Device Lett., vol. 9, pp. 136-138, 1988.
- [10] D. Delagebeaudeuf and N. T. Linh, "Metal-(n) AlGaAs-GaAs two dimensional electron gas FET," IEEE Trans. Electron Devices, vol. ED-29, pp. 955-960, 1982.
- [11] AN-JUI SHEY, WALTER H. KU, "An Analytical Current-Voltage Characteristics Model For High Electron Mobility Transistors Based on Nonlinear Charge Control Formulation," IEEE Trans. Electron Devices, vol. 36, NO. 10, Oct. 1989.
- [12] Lenka, T.R., Panda, A.K.: Characteristics study of 2DEG transport properties of AlGaIn/GaN and AlGaAs/GaAs-based HEMT.
- [13] M. Li and Y. Wang, "2-D analytical model for current-voltage characteristics and transconductance of AlGaIn/GaN MODFETs," IEEE Trans. Electron Devices, vol. 55, no. 1, pp. 261-267, Jan. 2008.
- [14] Sourabh Khandelwal, Nitin Goyal, and Tor A. Fjeldly, Fellow, IEEE, "A Physics Based Analytical Model For 2-DEG Charge Density In AlGaIn/GaN HEMT Devices," IEEE TRANSACTIONS ON ELECTRON DEVICES, VOL. 58, NO. 10, OCTOBER 2011.
- [15] Griff L. Bilbro, Senior Member, IEEE, and Robert J. Trew, Fellow, IEEE, "A Five-Parameter Model of the AlGaIn/GaN HFET," IEEE TRANSACTIONS ON ELECTRON DEVICES, VOL. 62, NO. 4, APRIL 2015.

- [16] Naveen Karumuri, Sreenidhi Turuvekere, Nandita DasGupta, Member, IEEE, and Amitava DasGupta, Member, IEEE, A Continuous Analytical Model for 2-DEG Charge Density in AlGa<sub>N</sub>/Ga<sub>N</sub> HEMTs Valid for All Bias Voltages IEEE TRANSACTIONS ON ELECTRON DEVICES, VOL. 61, NO. 7, JULY 2014.
- [17] [Sudip Ghosh, Avirup Dasgupta, Graduate Student Member, IEEE, Sourabh Khandelwal, Member, IEEE, Shantanu Agnihotri, and Yogesh Singh Chauhan, Senior Member, IEEE, Surface-Potential-Based Compact Modeling of Gate Current in AlGa<sub>N</sub>/Ga<sub>N</sub> HEMTs IEEE TRANSACTIONS ON ELECTRON DEVICES, VOL. 62, NO. 2, FEBRUARY 2015.](#)
- [18] [Sourabh Khandelwal fl, T.A. Fjeldly, Dept. of Electronics and Telecommunications, Norwegian University of Science and Technology, Norway, "A physics based compact model of I-V and C-V characteristics in AlGa<sub>N</sub>/Ga<sub>N</sub> HEMT Devices", Solid-State Electronics 76 \(2012\) 60–66.](#)
- [19] [N. A. Yuzeeva1 · A. V. Sorokoumova2 · R. A. Lunin2, L. N. Oveshnikov3 · G. B. Galiev1,4 · E. A. Klimov1 ,D. V. Lavruchin1 · V. A. Kulbachinskii2,3,4, "Electron Mobilities and Effective Masses in InGaAs/InAlAs HEMT Structures with High In Content" J Low Temp Phys DOI 10.1007/s10909-016-1589-6.](#)
- [20] I. Vurgaftman, J.R. Meyer, L.R. Ram-Mohan, J. Appl. Phys. 89, 5815 (2001)
- [21] S. Adachi, Properties of Group-IV, III-V and II-VI Semiconductors (Wiley, Chichester, 2005)
- [22] [A. Asgaria, M. Kalafia, and L. Faraone, "A quasi-two-dimensional charge transport model of AlGa<sub>N</sub>/Ga<sub>N</sub> high electron mobility transistors \(MODFETs\)," Physica E, vol. 28, no. 4, pp. 491–499, Sep. 2005.](#)
- [23] [Y. F. Wu, B. P. Keller, P. Fini, S. Keller, T. J. Jenkins, L.T.Kehias, S. P. Denbaares, and U. K. Mishra, "Bias dependent microwave performance of AlGa<sub>N</sub>/Ga<sub>N</sub> MODFETs up to 100 V," IEEE Electron Device Lett., vol. 18, no. 6, pp. 290–292, Jun. 1997.](#)
- [24] [Aixi Zhang, Student Member, IEEE, Lining Zhang, Member, IEEE, Zhikai Tang, Student Member, IEEE, Xiaoxu Cheng, Yan Wang, Kevin J. Chen, Fellow, IEEE, and Mansun Chan, Fellow, IEEE, Analytical Modeling of Capacitances for Ga<sub>N</sub> HEMTs, Including Parasitic Components, IEEE TRANSACTIONS ON ELECTRON DEVICES, VOL. 61, NO. 3, MARCH 2014.](#)
- [25] [R. Vetry, N. Q. Zhang, S. Keller, and U. K. Mishra, "The impact of surface states on the DC and RF characteristics of AlGa<sub>N</sub>/Ga<sub>N</sub> HFETs," IEEE Trans. Electron Devices, vol. 48, no. 3, pp. 560–566, Mar. 2001.](#)
- [26] [A. Koudymov, M. S. Shur, and G. Simin, "Compact model of current collapse in heterostructure field-effect transistors," IEEE Electron Device Lett., vol. 28, no. 5, pp. 332–335, May 2007.](#)
- [27] [X. Z. Dang et al., "Measurement of drift mobility in AlGa<sub>N</sub>/Ga<sub>N</sub> heterostructure field-effect transistor," Appl. Phys. Lett., vol. 74, no. 25, pp. 3890–3892, Jun. 1999.](#)
- [28] [Wu Y-F, Keller S, Kozodoy P, Keller BP, Kapolnek D, Denbaars SP, et al. Bias dependent microwave performance of AlGa<sub>N</sub>/Ga<sub>N</sub> MODFETs up to 100 V. IEEE Electron Dev Lett 1997;18\(6\):290–2.](#)
- [29] [Servin Rathi, Ritesh Gupta, Mridula Gupta and S. Gupta, "Comparative Subthreshold Analysis for Channel Thickness Variation on Sub-100 nm Double Gate with Single-Gate HEMT", Proceedings of International Conference on Microwave- 08.](#)
- [30] [Guohao Yu, Yue Wang, Yong Cai, Zhihua Dong, Chunhong Zeng, and Baoshun Zhang, Dynamic "Characterizations of AlGa<sub>N</sub>/Ga<sub>N</sub> HEMTs With Field Plates Using a Double-Gate Structure", IEEE ELECTRON DEVICE LETTERS, VOL. 34, NO. 2, FEBRUARY 2013.](#)
- [31] [S. Zafar\\* a, b\), A. Kashifa\), S. Hussain b\), N. Akhtar a\), N. Bhatti a\) and M. Imran a\), Designing of Double Gate HEMT in TCAD for THz Applications", Proceedings of 2013 10th International Bhurban Conference on Applied Sciences & Technology \(IBCAST\) Islamabad, Pakistan, 15th - 19th January, 2013.](#)
- [32] [Dong Seup Lee, Han Wang, Allen Hsu, Mohamed Azize, Oleg Laboutin, Yu Cao, Jerry Wayne Johnson, Edward Beam, Andrew Ketterson, Michael L. Schuette, Paul Saunier, Tomás Palacios, "Nanowire Channel InAlN/Ga<sub>N</sub> HEMTs With High Linearity of gm and fT", IEEE ELECTRON DEVICE LETTERS, VOL. 34, NO. 8, AUGUST 2013.](#)
- [33] [Wael Jatal, Uwe Baumann, Heiko O. Jacobs, Frank Schwier, Jörg Pezoldt, "Tri-Gate Al<sub>0.2</sub>Ga<sub>0.8</sub>N/AlN/Ga<sub>N</sub> HEMTs on SiC/Si-substrates", Materials Science Forum ISSN: 1662-9752, Vol. 858, pp 1174-1177.](#)